International Journal of
Molecular Sciences

MDPI

Article

C···O and Si···O Tetrel Bonds: Substituent Effects and Transfer of the SiF_3 Group

Zhihao Niu [1], Qiaozhuo Wu [1], Qingzhong Li [1,*] and Steve Scheiner [2,*]

[1] The Laboratory of Theoretical and Computational Chemistry, School of Chemistry and Chemical Engineering, Yantai University, Yantai 264005, China; nzh19981019@s.ytu.edu.cn (Z.N.); wqz1143280082@163.com (Q.W.)
[2] Department of Chemistry and Biochemistry, Utah State University, Logan, UT 84322, USA
* Correspondence: lqz@ytu.edu.cn (Q.L.); steve.scheiner@usu.edu (S.S.)

Abstract: The tetrel bond (TB) between 1,2-benzisothiazol-3-one-2-TF_3-1,1-dioxide (T = C, Si) and the O atom of pyridine-1-oxide (PO) and its derivatives (PO-X, X = H, NO_2, CN, F, CH_3, OH, OCH_3, NH_2, and Li) is examined by quantum chemical means. The Si···O TB is quite strong, with interaction energies approaching a maximum of nearly 70 kcal/mol, while the C···O TB is an order of magnitude weaker, with interaction energies between 2.0 and 2.6 kcal/mol. An electron-withdrawing substituent on the Lewis base weakens this TB, while an electron-donating group has the opposite effect. The SiF_3 group transfers roughly halfway between the N of the acid and the O of the base without the aid of cooperative effects from a third entity.

Keywords: noncovalent bonds; AIM; energy decomposition; charge transfer

check for updates

Citation: Niu, Z.; Wu, Q.; Li, Q.; Scheiner, S. C···O and Si···O Tetrel Bonds: Substituent Effects and Transfer of the SiF_3 Group. *Int. J. Mol. Sci.* **2023**, *24*, 11884. https://doi.org/10.3390/ijms241511884

Academic Editors: Nathan I. Hammer and Gregory Tschumper

Received: 15 June 2023
Revised: 19 July 2023
Accepted: 21 July 2023
Published: 25 July 2023

Copyright: © 2023 by the authors. Licensee MDPI, Basel, Switzerland. This article is an open access article distributed under the terms and conditions of the Creative Commons Attribution (CC BY) license (https://creativecommons.org/licenses/by/4.0/).

1. Introduction

The tetrel bond [1] (TB) is defined as an attractive interaction between the tetrel center (group 14 element) of an electron-deficient Lewis acid and an electron-rich Lewis base. TBs have an unparalleled importance in molecular recognition [2] and crystalline materials [3] since they can be used as a new molecular linker in crystal engineering. Therefore, the structure, strength, properties, and nature of TBs have been extensively studied [4–10]. When a tetrel atom is adjacent to an electron-withdrawing atom or group, a region with a positive electrostatic potential is found on its surface. When the tetrel atom is sp^3- and sp^2-hybridized, such regions are called σ-holes and π-holes, respectively [11,12]. Furthermore, sp^3-hybridized tetrels usually form weaker tetrel bonds than do sp^2-hybridized tetrels. In most cases, the tetrel bond magnifies in the order C << Si < Ge < Sn < Pb due to the fact that the higher the atomic number, the smaller the electronegativity, and the greater the polarization [11]. The carbon atom has difficulty in forming a TB unless it is attached to a strong electron-withdrawing group, or the Lewis base with which it interacts is particularly strong. For example, the methyl carbon atoms of CH_3OH and CH_3F can form weak tetrel bonds with some Lewis bases such as H_2O [13]. Although the tetrel bond involving the carbon donor is relatively weak, it plays an important role in protein–ligand systems [14,15] and chemical reactions [16].

Due to its greater electronegativity and lower polarizability, the carbon atom is rarely involved in strong TBs, which are also known as carbon bonds, if the carbon atom acts as a Lewis acid. Even so, carbon bonding has been observed in different systems. Weak Ar···C interactions were first detected in Ar···propynyl alcohol complexes by microwave spectroscopy and ab initio calculations [17]. Mani and Arunan carried out a theoretical study of carbon bonding in complexes of methanol and methyl fluoride, where the methyl group is attached to an electron-withdrawing group and placed in conjunction with a neutral base, finding interaction energies of ~2 kcal/mol [13]. The prevalence of such carbon bonding was further demonstrated in the solid state using the Cambridge Structural Database (CSD) and charge density analysis [18]. Similarly, the -CF_3 group in $ArCF_3$ is able

to participate in carbon bonding if the electron donor atom is not combined with active hydrogen atoms [19]. Otherwise, it favors the formation of weak hydrogen bonds through the F atoms [20].

The CF_3 group is common in drug molecules and it is involved in the recognition of the activity of medicament [21,22]. Thus, researchers have designed numerous trifluoromethylating reagents to introduce a CF_3 group into a target molecule [23–25]. It has been demonstrated that this group plays a dual function in noncovalent interactions since its C atom provides a σ-hole to join a tetrel bond and its F atoms are functioning electron donors [26]. There have been attempts to limit the group's function to only the TB. One approach is to select an electron donor such as NCLi without active hydrogen atoms to avoid the formation of a H-bond to F [4]. An alternate strategy involves deepening the σ-hole on the C atom, which can be realized by adding a positive charge to the tetrel donor molecule or adjoining an electron-withdrawing group to the C atom [13,20]. In tetrazole-CF_3···NCLi, where both methods were employed, a pure tetrel bond was achieved with an interaction energy of 3.79 kcal/mol [27].

In the protodesilylation reaction of phenyltrifluorosilane (PTS) with 8-hydroxyquinoline, a C–Si bond cleavage was found and the $–SiF_3$ group migrated from PTS to 8-hydroxyquinoline, resulting in a pentacoordinated silicon complex [28]. Such pentacoordinated silicon complexes have been synthesized and characterized [29–32]. They were thought to be an intermediate along the S_N2 reaction pathway and the authors pointed out that the nature of the leaving group is a key factor in determining the degree of Si–O bond formation [33]. Past work has considered the transfer of an sp^3-hybridized silicon group between two atoms that are facilitated by cooperativity with another interaction, such as the cation–π interaction, triel bond, and beryllium bond [27,34,35]. A major question emerges as to whether such a migration can occur without benefit of cooperativity engendered by a third unit.

In order to address this question, the present work begins with the construction of what may be a powerful tetrel-bonding C or Si atom. The NH hydrogen of the saccharin molecule is replaced by both a CF_3 and a SiF_3 group to compare C and Si in this regard. This molecule, designated here as S-TF_3, contains the elements of a strong TB, in that the N of the TF_3 group is attached to electron-withdrawing CO and SO_2 groups (see Figure 1). As a Lewis base partner, pyridine-1-oxide (PO) contains an O atom with a partial negative charge. The ability of this molecule to participate in a TB is modulated by placing various substituents at the position para to N-O. The list of substituents CH_3, OH, OCH_3, NH_2, Li, NO_2, CN, and F is of varying degrees of both electron-withdrawing and -donating potential so as to cover a wide gamut of base strength. Questions of interest first concern how the nature of each substituent affects both the C···O and Si···O tetrel bonds. How strong are these TBs and are they constituted of the same components as are generic noncovalent bonds? Another primary issue involves the possibility that either the CF_3 or SiF_3 group might transfer toward the O atom of the base, and by how much. Can such a transfer occur even in the absence of a third molecule and its cooperative influence?

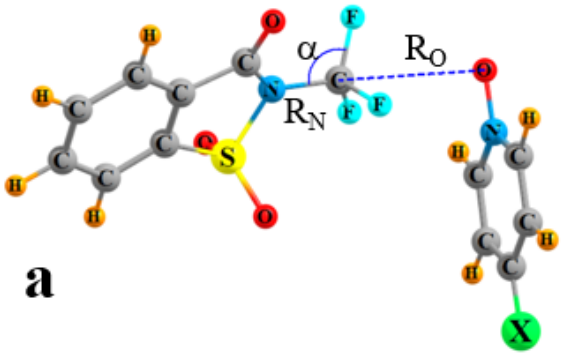

Figure 1. *Cont.*

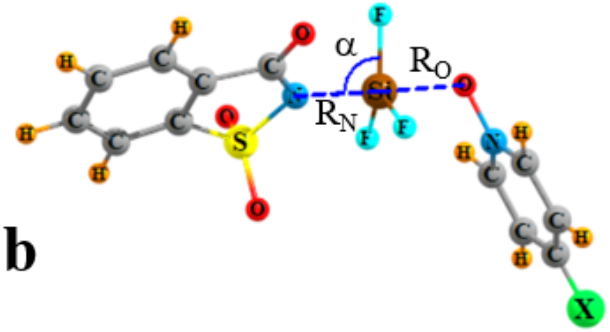

Figure 1. Geometries of complexes (**a**) S-CF_3 and (**b**) S-SiF_3 with PO-X bases, indicating definitions of geometrical parameters.

2. Theoretical Methods

The geometries of both monomers and complexes were optimized at the M06-2X/aug-cc-pVDZ level. This method has been used to study various tetrel-bonded complexes due to its accuracy and ability to incorporate dispersive effects [10,36,37]. All geometries corresponded to true minima on the potential energy surfaces since no imaginary frequencies were found when performing harmonic frequency calculations at the same level. The interaction energy (E_{int}) was calculated as the energy difference between the complex and the monomers frozen in their geometry within the complex. When the optimized geometries of monomers are utilized, this quantity equates to the binding energy (E_b). Both E_{int} and E_b were corrected for basis set superposition error (BSSE) using the method proposed by Boys and Bernardi [38]. All calculations were performed using the Gaussian 09 program [39].

The molecular electrostatic potential (MEP) for each monomer on a 0.001 a.u. isodensity surface was calculated at the M06-2X/aug-cc-pVDZ level using the wave function analysis surface analysis software (WFA-SAS) [40]. The electron density (ρ), Laplacian ($\nabla^2\rho$), and total energy density (H) at each bond critical point (BCP) were evaluated by the Multiwfn [41] procedure using Bader's atom-in-molecule (AIM) theory [42]. Charge transfer and orbital interactions between the electron donor and acceptor in the complexes were analyzed using the natural bond orbital (NBO) method [43]. The role of orbitals in the complexes was analyzed by the extended transition state–natural orbitals for chemical valence (ETS-NOCV) [44]. The interaction energy was decomposed into five physically significant components at the M06-2X/aug-cc-pVDZ level using the Local Molecular Orbital Energy Decomposition Analysis (LMOEDA) method [45] in the GAMESS program [46]: electrostatic energy (E^{es}), exchange energy (E^{ex}), repulsive energy (E^{rep}), polarization energy (E^{pol}), and dispersion energy (E^{disp}).

3. Results

The molecular electrostatic potential (MEP) of each of the monomers is illustrated in Figure 2. Of greatest importance is the positively charged σ-hole along the extension of the N-T bond axis of both S-CF_3 and S-SiF_3. The magnitude of the maximum of the MEP on the 0.001 au isodensity surface is equal to 13.8 and 40.8 kcal/mol, respectively, clearly much larger for the latter than for the C analog. The minimum of the MEP on each Lewis base occurs near its O atom and is equal to −40.8 kcal/mol for PO. Placing an electron-withdrawing group like CN or NO_2 on the ring pulls density away from the O, thereby reducing the magnitude of V_{min}. The reverse effect occurs for electron-donating substituents, which intensify this minimum. As may be seen by the V_{min} values listed in the first column of Table 1, this quantity ranges from −27.6 kcal/mol for PO-NO_2 to −55.2 kcal/mol for PO-Li.

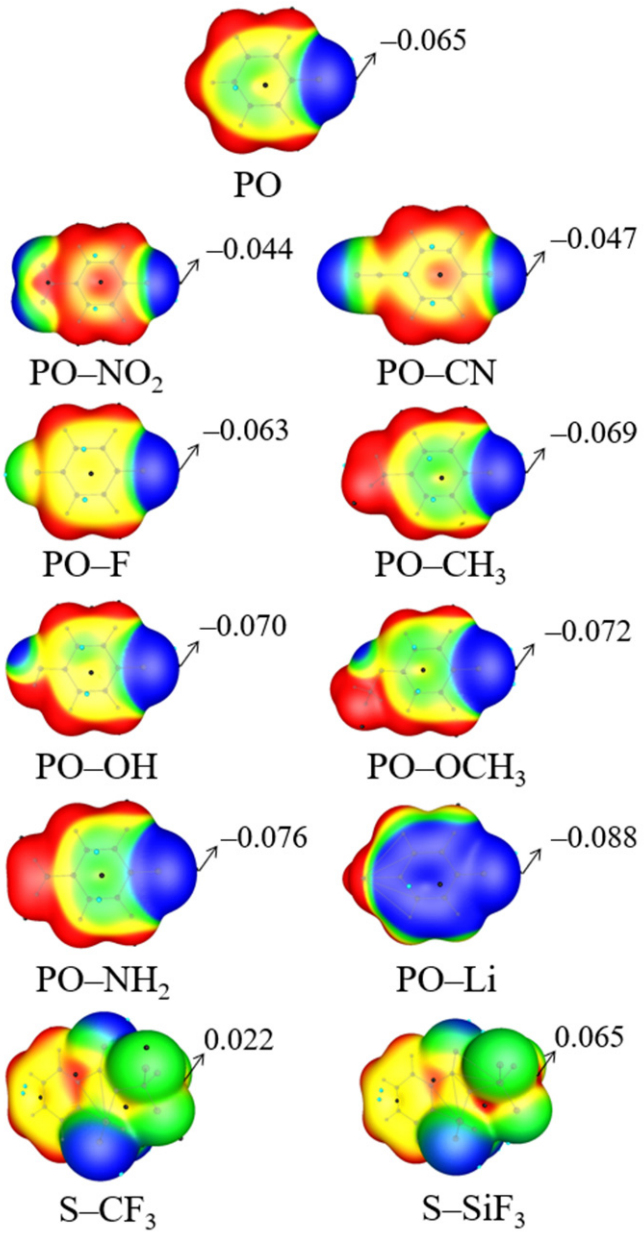

Figure 2. MEP maps of PO–X and S–TF_3 monomers. Color ranges in a.u: red, greater than 0.02; yellow, between 0.02 and 0; green, between −0.02 and 0; blue, less than −0.02.

The pairing of either S-CF_3 or S-SiF_3 with each of the various bases leads to geometries exemplified by Figure 1 wherein the O atom of the base approaches the C or Si atom to form a tetrel bond. The salient features of the structures of these complexes reported in the remainder of Table 1 display some overarching trends. In the first place, the Si···O TBs are considerably shorter than the C···O bonds. The R_O distances from T to O in the former are all less than 2.0 Å, while they exceed 3.0 Å in the latter. Concomitant with the shorter Si···O TBs is a much greater elongation of the internal R(N···T) distance R_N, which is roughly 0.1 Å, as compared to those for C···O that are an order of magnitude smaller. Indeed, the R_O/R_N ratio is nearly unity for the Si···O interactions, signifying that the SiF_3 group lies roughly midway between the N and O atoms. Along with what may be thought of as a half transfer, there is a flattening of the SiF_3 group, in that the α angle in Figure 1 lowers from tetrahedral for the weak C···O interactions to nearly 90° for Si···O.

Table 1. Minima in MEP of Lewis bases (V_{min}, kcal/mol), T···O distance (R_O, Å), N-T bond length (R_N, Å), and its change (ΔR_N) relative to the monomer, average of three N-T-F angles (α, deg) in the complexes.

	V_{min}	R_O	R_N	ΔR_N	R_O/R_N	γ_O [a]	γ_N [a]	α
S-CF_3···PO-NO_2	−27.6	3.123	1.431	0.005	2.183	0.970	0.441	110.2
S-CF_3···PO	−40.8	3.151	1.436	0.010	2.193	0.979	0.442	109.9
S-CF_3···PO-CH_3	−43.3	3.119	1.437	0.011	2.169	0.969	0.442	109.8
S-CF_3···PO-OH	−43.9	3.115	1.437	0.011	2.169	0.967	0.442	109.8
S-CF_3···PO-OCH_3	−45.2	3.144	1.437	0.011	2.188	0.976	0.442	109.8
S-CF_3···PO-NH_2	−47.7	3.085	1.438	0.012	2.146	0.958	0.442	109.7
S-CF_3···PO-Li	−55.2	3.097	1.440	0.014	2.151	0.962	0.443	109.6
S-SiF_3···PO-NO_2	−27.6	1.902	1.819	0.080	1.045	0.526	0.499	94.3
S-SiF_3···PO-CN	−29.5	1.896	1.821	0.082	1.042	0.524	0.499	94.2
S-SiF_3···PO-F	−39.5	1.874	1.829	0.090	1.025	0.518	0.501	93.5
S-SiF_3···PO	−40.8	1.874	1.831	0.092	1.024	0.518	0.502	93.3
S-SiF_3···PO-CH_3	−43.3	1.866	1.834	0.095	1.017	0.515	0.502	93.1
S-SiF_3···PO-OH	−43.9	1.860	1.834	0.095	1.014	0.514	0.502	93.0
S-SiF_3···PO-OCH_3	−45.2	1.856	1.836	0.097	1.011	0.513	0.503	92.9
S-SiF_3···PO-NH_2	−47.7	1.848	1.841	0.102	1.004	0.510	0.504	91.2
S-SiF_3···PO-Li	−55.2	1.842	1.849	0.110	0.996	0.509	0.507	92.2

[a] γ is the ratio of R_O or R_N to the sum of the van der Waals radii of the two atoms.

As a finer point, it may be noted that there is a relationship between the strength of the nucleophile as measured by its V_{min} and the geometric quantities. As this minimum intensifies, there is a general tendency for the TB to shorten, as is evident in the R_O quantities in Table 1. This contraction of TB induces an enhanced elongation of the internal R-N, ΔR_N, as well as more flattening of the TF_3 group as measured by α.

The interaction energy of each dimer E_{int} compares the energy of the complex with the sum of the individual monomers, held within their internal geometries they attain within the dimer. The binding energy E_b takes the fully optimized separated monomers as its reference point, so corresponds to the dimerization reaction energy. These two quantities differ by the energy DE required to deform each monomer into its geometry within the dimer.

All of these quantities are contained in Table 2 for each of the complexes and are reflective of the geometrical trends in Table 1. The interaction and binding energies of the C···O tetrel bonds in the upper half of Table 2 are only about 2–3 kcal/mol, consistent with the lengths of these weak intermolecular bonds that are greater than 3.0 Å. The highly compact Si···O complexes contain much stronger bonds. Interaction energies range from 47 to 69 kcal/mol. Due to the distortion of the monomers incurred by the dimerization, with deformation energies between 30 and 40 kcal/mol, the binding energies are reduced to the 15–30 kcal/mol range, but still fall into the category of strong interactions. There is a strong correlation between the interaction energies and the Si···O separations, as exhibited in Figure S1 with a correlation coefficient of 0.99. Although imperfect, there is also a correlation observed between the interaction energetics and the minimum in the Lewis base's MEP. As illustrated in Figure S2, this relationship is nearly linear with a correlation coefficient of 0.97 for the Si series.

One tool to better understand the nature and strength of these bonds arises in the context of AIM analysis of the electron density topology. The data reported in Table 3 refer to the bond critical points that lie roughly midway between the T atom and the O and N centers with which it interacts. In the case of the very weak tetrel bonds in the CF_3 cases, the AIM procedure fails to locate a bond path between C and O, finding instead three paths from O to F, as pictured in Figure S3. This topology is reminiscent of other tetrel bonds involving $–CF_3$ [4]. On the other hand, it is important to note that NBO analysis affirms the presence of a TB. In the S-CF_3···PO system, a charge transfer from the O lone pair of PO to the σ*(NC) antibonding orbital of S-CF_3 is signaled by NBO via a second-order

perturbation energy E^2 of 0.35 kcal/mol, larger than any of the values corresponding to transfers to C-F antibonding orbitals. The situation is quite different for the SiF_3 complexes in the lower half of Table 3. In the first place, there is a clear bond path connecting Si with O (see Figure S3), and its critical point density is between 0.07 and 0.08 au, an order of magnitude larger than in CF_3.

Table 2. Interaction energy (E_{int}), binding energy (E_b), and deformation energy (DE) in the complexes, all in kcal/mol.

	E_{int}	E_b	DE
S-CF_3···PO-NO_2	−2.69	−2.55	0.14
S-CF_3···PO	−2.33	−2.12	0.21
S-CF_3···PO-CH_3	−2.36	−2.13	0.23
S-CF_3···PO-OH	−2.63	−2.35	0.28
S-CF_3···PO-OCH_3	−2.62	−2.36	0.26
S-CF_3···PO-NH_2	−2.37	−2.11	0.26
S-CF_3···PO-Li	−2.01	−1.62	0.39
S-SiF_3···PO-NO_2	−46.59	−15.12	31.47
S-SiF_3···PO-CN	−48.12	−16.29	31.83
S-SiF_3···PO-F	−56.59	−22.39	34.20
S-SiF_3···PO	−56.45	−21.82	34.63
S-SiF_3···PO-CH_3	−59.29	−23.78	35.51
S-SiF_3···PO-OH	−61.52	−25.64	35.88
S-SiF_3···PO-OCH_3	−62.65	−26.29	36.36
S-SiF_3···PO-NH_2	−66.58	−28.50	38.08
S-SiF_3···PO-Li	−69.15	−29.76	39.39

Table 3. Electron densities (ρ), Laplacians ($\nabla^2\rho$), and energy densities (H) at the T···O and N-T BCPs in the complexes, all in a.u.

	T···O [a]			N-T		
	ρ	**$\nabla^2\rho$**	**H**	**ρ**	**$\nabla^2\rho$**	**H**
S-CF_3···PO-NO_2	0.0067	0.0372	0.0018	0.2926	−0.8536	−0.3242
S-CF_3···PO	0.0072	0.0390	0.0016	0.2894	−0.8362	−0.3191
S-CF_3···PO-CH_3	0.0074	0.0403	0.0016	0.2885	−0.8316	−0.3177
S-CF_3···PO-OH	0.0066	0.0361	0.0018	0.2885	−0.8312	−0.3176
S-CF_3···PO-OCH_3	0.0066	0.0357	0.0017	0.2882	−0.8294	−0.3169
S-CF_3···PO-NH_2	0.0078	0.0423	0.0017	0.2876	−0.8271	−0.3166
S-CF_3···PO-Li	0.0071	0.0388	0.0018	0.2853	−0.8170	−0.3142
S-SiF_3···PO-NO_2	0.0707	0.3233	−0.0162	0.1004	0.4831	−0.0279
S-SiF_3···PO-CN	0.0716	0.3317	−0.0162	0.1000	0.4796	−0.0278
S-SiF_3···PO-F	0.0758	0.3686	−0.0163	0.0982	0.4656	−0.0272
S-SiF_3···PO	0.0756	0.3680	−0.0161	0.0976	0.4612	−0.0269
S-SiF_3···PO-OH	0.0783	0.3917	−0.0163	0.0969	0.4551	−0.0267
S-SiF_3···PO-NH_2	0.0808	0.4139	−0.0164	0.0955	0.4444	−0.0263
S-SiF_3···PO-OCH_3	0.0790	0.3990	−0.0162	0.0965	0.4524	−0.0266
S-SiF_3···PO-NH_2	0.0808	0.4139	−0.0164	0.0955	0.4444	−0.0263
S-SiF_3···PO-Li	0.0815	0.4247	−0.0161	0.0937	0.4308	−0.0257

[a] Topological parameters at the intermolecular BCP in the S-CF_3 complexes were obtained as the sum of three F···O BCPs.

It is the sum of these three AIM quantities that are reported in the upper half of Table 3. Even with three separate terms contributing, the total of these three densities remains well below 0.01 au and the sum of the three energy densities is likewise quite small. The contrast with the far larger quantities on the right side of Table 3 is striking, with all indicating a strong covalent bond. The densities of the N-T bond in the SiF_3 complexes drop significantly compared to CF_3, down to around 0.10 au, a bit larger than the Si···O quantities. The magnitudes of the three AIM properties contained in Table 3

are consistent with a strong noncovalent bond, with a certain degree of covalency [47]. In terms of patterns, the AIM quantities for the Si···O bonds tend to rise as the substituent on the PO becomes more electron-donating, consistent with the geometric and energetic trends mentioned above.

An important component of the TB and related covalent bonds is the transfer of a certain amount of charge from the electron donor unit to the acceptor. The first column of Table 4 shows that the amount of this transfer (CT) is very small in the S-CF_3 complexes, 0.001 e or less. But the transfer is greatly magnified in the SiF_3 complexes approaching and surpassing 0.2 e. As in the case of the previous parameters, CT also rises as the PO substituent becomes more electron-donating toward the bottom of Table 4. This amount is greatly amplified in the S-SiF_3 system, all close to 0.2 e. For each series of complex, whether S-CF_3 or S-SiF_3, CT follows a similar pattern with the interaction energy since both terms have a good linear relationship (Figure S4). In fact, Figure S4 documents a close linear relationship between CT and E_{int}, with a correlation coefficient of 0.99 for the Si systems.

Table 4. Charge transfer (CT, e) and NOCV orbital energies (E, kcal/mol) in the complexes.

	CT [a]	E
S-CF_3···PO-NO_2	0.0013	−0.31
S-CF_3···PO	0.0009	−0.36
S-CF_3···PO-CH_3	0.0004	−0.39
S-CF_3···PO-OH	0.0001	−0.39
S-CF_3···PO-OCH_3	0.0006	−0.39
S-CF_3···PO-NH_2	0.0005	−0.44
S-CF_3···PO-Li	0.0002	−0.43
S-SiF_3···PO-NO_2	0.1755	−54.50
S-SiF_3···PO-CN	0.1780	−55.26
S-SiF_3···PO-F	0.1900	−58.50
S-SiF_3···PO	0.1907	−58.67
S-SiF_3···PO-CH_3	0.1942	−60.00
S-SiF_3···PO-OH	0.1961	−60.58
S-SiF_3···PO-OCH_3	0.1977	−61.20
S-SiF_3···PO-NH_2	0.2024	−62.59
S-SiF_3···PO-Li	0.2059	−64.08

[a] Sum of natural atomic charges of PO-X subunit.

The strong covalent elements in the bonds within the S-SiF_3···PO-X dimers precludes the usefulness of the NBO to extract the charge transfer between the N lone pair of PO-X and the σ*(N-Si) antibonding orbital [27] since the NBO views these complexes as a single molecular entity. Another useful tool that can be applied here derives from the Natural Orbitals for Chemical Valence (NOCV) approach. The isosurface of the NOCV pair density maps of S-CF_3···PO and S-SiF_3···PO is shown in Figure 3 as illustrative cases. The shapes of these density shift orbitals are similar but there is obviously a larger magnitude for the latter case. This idea of a larger magnitude carries over to the energies of the corresponding NOCV orbital energies listed in the last column of Table 4. In fact, an excellent linear relationship is found between the NOCV orbital energy and the full interaction energy, as evident by the correlation coefficient of 0.99 in Figure S5.

As another window into the nature of the T···O TB, the interaction energy of each complex is decomposed into five terms, including electrostatic (E^{es}), exchange (E^{ex}), repulsion (E^{rep}), polarization (E^{pol}), and dispersion (E^{disp}). As is clear from Table 5, the largest contributor to the weak C···O TBs is the dispersion energy, which amounts to some 9 kcal/mol. The electrostatic and exchange terms are considerably smaller, and the polarization energy is only 1 kcal/mol. The magnitudes of these terms are much larger in the SiF_3 systems. The dispersion energy climbs to nearly 30 kcal/mol but is superseded by the other contributors. The polarization energy rises to the 63–77 kcal/mol range, and the exchange energy is roughly 60 kcal/mol. The largest contribution originates in the electrostatic contribution, which amounts to some 75–100 kcal/mol. The near-dominance by E^{es} is consistent with the

close correlation between the interaction energy and the minimum of the base's MEP. But each of the various attractive terms is in good coincidence with the full interaction energy, as shown by the linear relationships in Figure S6, with correlation coefficients of E^{es}, E^{pol}, and E^{disp} equal to 0.98, 0.99, and 0.97, respectively.

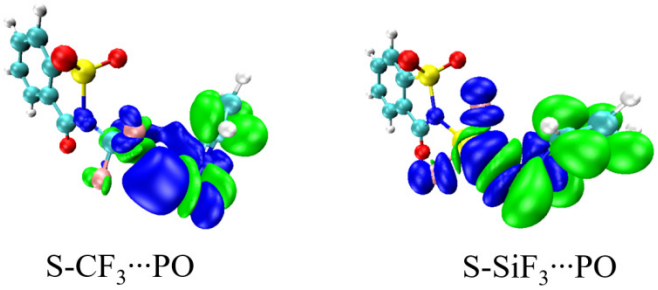

Figure 3. Isosurface of NOCV pair density map of S-CF_3···PO and S-SiF_3···PO.

Table 5. Electrostatic (E^{es}), exchange (E^{ex}), repulsion (E^{rep}), polarization (E^{pol}), and dispersion energies (E^{disp}), as well as the total interaction energy (ΔE^{total}) in the complexes. All in kcal/mol.

	E^{es}	E^{ex}	E^{rep}	E^{pol}	E^{disp}	ΔE^{total}
S-CF_3···PO-NO_2	−3.61	−2.77	12.79	−0.74	−8.45	−2.78
S-CF_3···PO	−3.37	−3.12	13.68	−0.88	−8.69	−2.38
S-CF_3···PO-CH_3	−3.50	−3.30	14.17	−1.03	−8.76	−2.42
S-CF_3···PO-OH	−3.70	−3.23	13.92	−1.04	−8.68	−2.73
S-CF_3···PO-OCH_3	−3.64	−3.26	14.11	−1.05	−8.86	−2.70
S-CF_3···PO-NH_2	−3.80	−3.69	15.17	−1.14	−8.95	−2.42
S-CF_3···PO-Li	−2.97	−3.28	13.73	−1.24	−8.31	−2.06
S-SiF_3···PO-NO_2	−74.86	−54.07	169.62	−63.03	−26.97	−49.31
S-SiF_3···PO-CN	−76.91	−54.94	172.17	−64.04	−27.17	−50.89
S-SiF_3···PO-F	−88.66	−59.35	185.02	−68.96	−27.67	−59.62
S-SiF_3···PO	−87.17	−58.59	182.73	−68.78	−27.68	−59.51
S-SiF_3···PO-CH_3	−90.66	−59.97	186.83	−70.93	−27.75	−62.48
S-SiF_3···PO-OH	−94.57	−61.55	191.51	−72.18	−27.92	−64.72
S-SiF_3···PO-OCH_3	−95.80	−62.06	193.06	−73.16	−27.90	−65.85
S-SiF_3···PO-NH_2	−100.42	−63.69	197.82	−75.37	−28.25	−69.91
S-SiF_3···PO-Li	−100.95	−63.45	196.96	−77.16	−28.09	−72.69

4. Discussion

The forgoing data have documented that the formation of each complex elongates the internal R(N-T) distance within the S-TF_3 subunit. While this stretch is only about 0.01 Å for T = C, it approaches 0.10 Å for the S-SiF_3 systems. Given the roughly half transfer of the SiF_3 groups in the latter complexes, one can take an alternate perspective and consider the stretch of the Si-O bond, from an imagined endpoint involving full transfer to the PO-X. The monomer resulting from this transfer depends upon whether the SiF_3 group is electrically neutral or bears a positive charge, corresponding roughly to either a H atom or proton transfer within a H-bonded complex. Taking the unsubstituted PO unit as an example, the O-Si distance in the neutral SiF_3-PO unit is optimized to 1.661 Å, while this same bond length is 1.703 Å in the cation. Since the Si···O distance within the S-SiF_3···PO complex is shown to be 1.874 Å in Table 1, the latter distance can be considered a stretch of 0.213 Å relative to the neutral, and 0.171 Å with respect to the cationic monomer. Both of these stretches are somewhat larger than the elongation of the N-Si bond of 0.092 Å relative to the S-SiF_3 monomer. So, from this geometrical perspective, the degree of SiF_3 transfer can be thought of as roughly 30% for the former neutral case and 35% for the cation transfer.

In biological and organic molecules, alkyl groups are commonly bonded to electronegative atoms. Hence, the interactions involving these alkyl groups, although individually weak, may be commonplace and together play an important cumulative role in the overall

structure and function [13]. It is known that the transition state of S_N2 reactions usually involves a quasi-pentacoordinate C interacting with two nucleophilic groups, so carbon bonding may facilitate this class of reaction [4]. This idea has motivated some of the attention that has lately been paid to the carbon bonding of methyl groups [13,19,48,49]. A consensus has been reached that C-bonding of any strength requires the presence of at least one electron-withdrawing substituent on the Lewis acid. The replacement of the three H atoms of CH_3 by F does not guarantee a deeper σ-hole nor a stronger tetrel bond [27], which may be due to the repulsion between the three F atoms and the electron donor atom. The choice of saccharin (1,2-benzisothiazol-3(2H)-one-1,1-dioxide) as the unit to which the TF_3 group is attached here is guided in part by the presence of two electron-withdrawing groups (carbonyl and sulfonyl) attached to the N atom, which is itself electronegative [27]. These factors contribute to the deep σ-hole on C for which V_{max} is 13.8 kcal/mol, and 40.8 if C is replaced by Si. In fact, the calculations delineated here verify that a tetrel bond is formed between the CF_3 group and the PO derivatives, with interaction energies between 2 and 3 kcal/mol.

Of course, bonds of this type can be magnified by charge assistance. That is, if the Lewis acid containing $–CF_3$ is positively charged [27] or the electron donor is an anion [50,51], the tetrel bond formed would be strengthened, with past results leading to values in the 7–8 kcal/mol range. A less extreme bond strengthening occurs if the base is enhanced by a strong electron donor as in the case of the metal atoms of NCLi and NCNa [4,27], in which case the C···N TB involving a CF_3 group rises up to about 4 kcal/mol. The choice of pyridine-1-oxide (PO) and its derivatives as a Lewis base here is made in part due to the strong potential of N-oxides as an electron donor. For example, past work found an interaction energy of 52 kcal/mol [52] upon pairing H_3NO with $PhSiF_3$ and $PhSiH_3$.

Whereas the mutation of the $–CH_3$ electron acceptor to $–CF_3$ does not necessarily strengthen the TB [27], the analogous fluorination of SiH_3 does so, as, for example, the rise in the bond strength by 33 kcal/mol when H_3NO acts as electron donor [52]. When a series of anions F^-, Cl^-, Br^-, CN^-, NC^-, N_3^-, NCS^-, and SCN^- bind with $NCCF_3$ and $NCSiF_3$ through a tetrel bond, the increase in interaction energy lies in the range of 18–75 kcal/mol when the C of $NCCF_3$ is changed to Si in $NCSiF_3$ [51]. With neutral PO-X as an electron donor, the TB strengthening on going from C to Si ranges from 44 to 67 kcal/mol.

The presence of a σ-hole on the tetrel atom can offer a reliable prediction for the formation of a tetrel bond, but its magnitude does not always correspond accurately with the bond strength. For example, in tetrel-bonded complexes of formamidine with TH_3F (T = C, Si, Ge, and Sn), the interaction energy increases in the order C < Ge < Si < Sn, inconsistent with the depth of the σ-hole on the T atom [53]. Similarly, while the negative MEP on the electron donor atom is predictive of its ability to form a tetrel bond, there are exceptions. The top half of Table 2 provides a case in point where the interaction energies do not follow the same pattern as does V_{min} for the S-CF_3···PO-X complexes. This inconsistency fits with prior reports of the tetrel-bonded complexes of TF_4 (T = Si, Ge, and Sn) with pyrazine and HCN [54], as well as in the halogen-bonded complexes of CF_3Cl with methylated amines [55]. In the case considered here, the inconsistency may be partly attributed to the stabilizing interactions other than the TB, which are marked by the AIM bond paths to the F atoms.

As described above, an electron-withdrawing substituent placed on the PO-X Lewis base attenuates its V_{max}, while the opposite occurs for an electron-donating X. This trend bears a direct consequence for the interaction energy. Figure 4 plots E_{int} for the S-SiF_3···POX systems against the aromatic substituent constant (δ) in a pair of Hammett plots, which document the strong relationship between these two parameters. It is hoped that a similar correlation can be helpful in estimating the strength of similar bonds in other types of noncovalent interactions, tetrel bonds or otherwise [56]. It is worth noting that an analogous relationship has been reported for the substituents in the Lewis acid molecule [57].

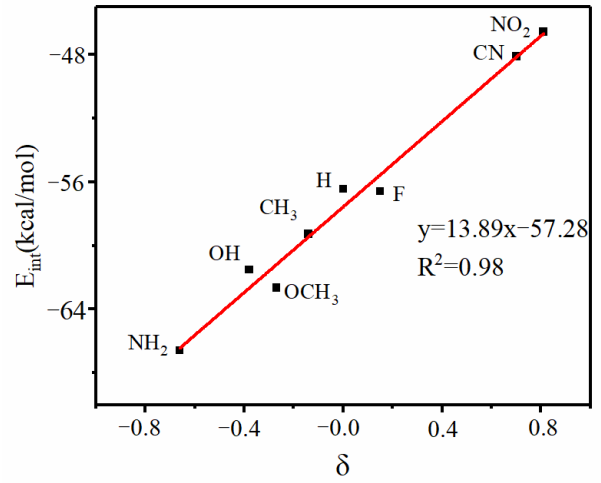

Figure 4. Hammett plots of S-SiF_3···POX complexes.

Because of its strong electron-releasing characteristic, the Li substituent leads to the strongest tetrel bonding enhancement when placed on the Lewis base. Extrapolating this idea, an alkali metal substituent may make the methyl C atom nucleophilic [9]. It stands to reason that two alkali metal atoms would make this enhancing effect even more prominent. To substantiate this idea, the interaction energy between CH_3F and C_2H_2 is only 1 kcal/mol, but two Li/Na substituents elevate this quantity by a factor of 5 to 5–6 kcal/mol [58]. Of course, other metals also have a similar effect. The tetrel bond formed between NCH and SiF_4 is weak with an interaction energy of 3.45 kcal/mol, but is increased nearly fourfold by the change from NCH to NCAg [59].

Our own group has been attracted to the question as to whether and under what circumstances a TR_3 group may be transferred across a tetrel bond, given its relevance to the S_N2 reaction and its significance in biological systems. It was learned that N-heterocyclic carbene ($C_3N_2H_4$, NHC) is a good electron donor in a tetrel bond (the interaction energy amounts to 26 kcal/mol with SiH_3F as the Lewis acid) [60], but NHC forms a weak tetrel bond (3.9 kcal/mol) with $PhSiH_3$ [34]. If Be^{2+} is added above the ring plane, resulting in a cation–π interaction, the interaction energy rises to 100 kcal/mol, and this strong tetrel bond results in the displacement of the $–SiH_3$ group from the C atom to N [34]. A similar cooperative effect occurs with a triel bond that can also aid in this transfer [27]. In the binary complexes between TF_3OH (T = Si and Ge) and Lewis base NCM (M = Li and Na), a half-transfer of $–TF_3$ occurs when a third $BeCl_2$ molecule approaches the O atom of TF_3OH and a fourth NCM molecule is introduced simultaneously [35]. The aforementioned transfers all rely on the cooperativity of the tetrel bond with other noncovalent interactions. The results described above deviate from this pattern in that the SiF_3 transfer occurs without need of the cooperativity of a third unit. This phenomenon may be due in part to the weakness of the internal N-Si bond in comparison to Si-O, coupled with the presence of the electron-withdrawing groups on the Lewis acid. This promotion is coupled with the strong nucleophilic characteristic of the N-oxide of the base used here.

5. Conclusions

A tetrel bond is formed between the O atom of pyridine-1-oxide (PO) and the tetrel atom T, either C or Si, on 1,2-benzisothiazol-3-one-2-TF_3-1,1-dioxide. Electron-withdrawing substituents placed on the former tend to weaken this TB as they make the electron pair of the donor O less accessible; the reverse occurs for electron-donating groups. The Si···O TBs are far stronger than their C···O analogs, reaching up toward 70 kcal/mol. Formation of the C···O TB amounts to less than 3 kcal/mol and, occasionally, a small stretch of the internal N-C covalent bond. The Si···O interaction is strong enough that the SiF_3 unit translates to a position roughly halfway between the N and O atoms.

Supplementary Materials: The following supporting information can be downloaded at: https://www.mdpi.com/article/10.3390/ijms241511884/s1.

Author Contributions: Conceptualization, Q.L.; methodology, Z.N. and Q.W.; software, Q.L.; validation, Z.N., Q.W. and Q.L.; formal analysis, Z.N. and Q.W.; investigation, Z.N. and Q.W.; resources, Q.L.; data curation, Z.N. and Q.W.; writing—original draft preparation, Z.N. and Q.W.; writing—review and editing, Q.L. and S.S.; visualization, Z.N. and Q.W.; supervision, Q.L. and S.S.; project administration, Q.L.; funding acquisition, Q.L. and S.S. All authors have read and agreed to the published version of the manuscript.

Funding: This work was supported by the Natural Science Foundation of Shandong Province (ZR2021MB123) and the US National Science Foundation (1954310).

Institutional Review Board Statement: Not applicable.

Informed Consent Statement: Not applicable.

Data Availability Statement: The data that support the findings of this study are available within the article and its Supplementary Material.

Conflicts of Interest: The authors declare no conflict of interest.

References

1. Bauzá, A.; Mooibroek, T.J.; Frontera, A. Tetrel-Bonding Interaction: Rediscovered Supramolecular Force? *Angew. Chem. Int. Ed.* **2013**, *52*, 12317–12321. [CrossRef] [PubMed]
2. Bauzá, A.; Ramis, R.; Frontera, A. Computational Study of Anion Recognition Based on Tetrel and Hydrogen Bonding Interaction by Calix [4] Pyrrole Derivatives. *Comput. Theor. Chem.* **2014**, *1038*, 67–70. [CrossRef]
3. Bauzá, A.; Mooibroek, T.J.; Frontera, A. Tetrel Bonding Interactions. *Chem. Rec.* **2016**, *16*, 473–487. [CrossRef]
4. Grabowski, S.J. Tetrel Bond–σ-Hole Bond as a Preliminary Stage of the S_N2 Reaction. *Phys. Chem. Chem. Phys.* **2014**, *16*, 1824–1834. [CrossRef] [PubMed]
5. Southern, S.A.; Bryce, D.L. NMR Investigations of Noncovalent Carbon Tetrel Bonds. Computational Assessment and Initial Experimental Observation. *J. Phys. Chem. A* **2015**, *119*, 11891–11899. [CrossRef]
6. Liu, M.X.; Li, Q.Z.; Cheng, J.B.; Li, W.Z.; Li, H.B. Tetrel Bond of Pseudohalide Anions with XH_3F (X = C, Si, Ge, and Sn) and its Role in S_N2 Reaction. *J. Chem. Phys.* **2016**, *145*, 224310. [CrossRef]
7. Scheiner, S. Systematic Elucidation of Factors That Influence the Strength of Tetrel Bonds. *J. Phys. Chem. A* **2017**, *121*, 5561–5568. [CrossRef]
8. Grabowski, S.J. Tetrel Bonds with π-Electrons Acting as Lewis Bases—Theoretical Results and Experimental Evidences. *Molecules* **2018**, *23*, 1183. [CrossRef]
9. Scheiner, S. The Ditetrel Bond: Noncovalent Bond between Neutral Tetrel Atoms. *Phys. Chem. Chem. Phys.* **2020**, *22*, 16606–16614. [CrossRef]
10. Scheiner, S. Relative Strengths of a Pnicogen and a Tetrel Bond and Their Mutual Effects upon One Another. *J. Phys. Chem. A* **2021**, *125*, 2631–2641. [CrossRef]
11. Murray, J.S.; Lane, P.; Politzer, P. Expansion of the σ-Hole Concept. *J. Mol. Model.* **2009**, *15*, 723–729. [CrossRef] [PubMed]
12. de Paul N. Nziko, V.; Scheiner, S. Comparison of π-Hole Tetrel Bonding with σ-Hole Halogen Bonds in Complexes of XCN (X = F, Cl, Br, I) and NH_3. Phys. *Chem. Chem. Phys.* **2016**, *18*, 3581–3590. [CrossRef]
13. Mani, D.; Arunan, E. The X–C···Y (X = O/F, Y = O/S/F/Cl/Br/N/P) 'Carbon Bond' and Hydrophobic Interactions. *Phys. Chem. Chem. Phys.* **2013**, *15*, 14377–14383. [CrossRef] [PubMed]
14. Mundlapati, V.R.; Sahoo, D.K.; Bhaumik, S.; Chandrakar, A.; Jena, S.; Biswal, H.S. Noncovalent Carbon-Bonding Interactions in Proteins. *Angew. Chem. Int. Ed.* **2018**, *57*, 16496–16500. [CrossRef] [PubMed]
15. García-Llinás, X.; Bauzá, A.; Seth, S.K.; Frontera, A. Importance of R–CF_3···O Tetrel Bonding Interactions in Biological Systems. *J. Phys. Chem. A* **2017**, *121*, 5371–5376. [CrossRef]
16. Karim, A.; Schulz, N.; Andersson, H.; Nekoueishahraki, B.; Carlsson, A.C.C.; Sarabi, D.; Valkonen, A.; Rissanen, K.; Gräfenstein, J.; Keller, S.; et al. Carbon's Three-Center, Four-Electron Tetrel Bond, Treated Experimentally. *J. Am. Chem. Soc.* **2018**, *140*, 17571–17579. [CrossRef]
17. Mani, D.; Arunan, E. Microwave Spectroscopic and Atoms in Molecules Theoretical Investigations on the Ar···Propargyl Alcohol Complex: Ar···H-O, Ar···π, and Ar···C Interactions. *ChemPhysChem* **2013**, *14*, 754–763. [CrossRef]
18. Thomas, S.P.; Pavan, M.S.; Row, T.N.G. Experimental Evidence for 'Carbon Bonding' in the Solid State from Charge Density Analysis. *Chem. Commun.* **2014**, *50*, 49–51. [CrossRef]
19. Bauzá, A.; Mooibroek, T.J.; Frontera, A. Non-Covalent sp^3 Carbon Bonding with $ArCF_3$ is Analogous to CH–π Interactions. *Chem. Commun.* **2014**, *50*, 12626–12629. [CrossRef]
20. Liu, M.; Li, Q.Z.; Scheiner, S. Comparison of Tetrel Bonds in Neutral and Protonated Complexes of PyridineTF_3 and FuranTF_3 (T = C, Si, and Ge) with NH_3. Phys. *Chem. Chem. Phys.* **2017**, *19*, 5550–5559. [CrossRef]

21. Meanwell, N.A. Synopsis of Some Recent Tactical Application of Bioisosteres in Drug Design. *J. Med. Chem.* **2011**, *54*, 2529–2591. [CrossRef] [PubMed]
22. Purser, S.; Moore, P.R.; Swallow, S.; Gouverneur, V. Fluorine in Medicinal Chemistry. *Chem. Soc. Rev.* **2008**, *37*, 320–330. [CrossRef]
23. Chen, Y.; Ma, G.; Gong, H. Copper-Catalyzed Reductive Trifluoromethylation of Alkyl Iodides with Togni's Reagent. *Org. Lett.* **2018**, *20*, 4677–4680. [CrossRef]
24. Zhang, M.; Lin, J.H.; Xiao, J.C. A Readily Available Trifluoromethylation Reagent and Its Difunctionalization of Alkenes. *Org. Lett.* **2021**, *23*, 6079–6083. [CrossRef] [PubMed]
25. Kalim, J.; Duhail, T.; Le, T.N.; Vanthuyne, N.; Anselmi, E.; Togni, A.; Magnier, E. Merging Hypervalent Iodine and Sulfoximine Chemistry: A New Electrophilic Trifluoromethylation Reagent. *Chem. Sci.* **2019**, *10*, 10516–10523. [CrossRef]
26. Hof, F.; Scofield, D.M.; Schweizer, W.B.; Diederich, F. A Weak Attractive Interaction between Organic Fluorine and an Amide Group. *Angew. Chem. Int. Ed.* **2004**, *43*, 5056–5059. [CrossRef]
27. Wu, Q.Z.; Xie, X.Y.; Li, Q.Z.; Scheiner, S. Enhancement of Tetrel Bond Involving Tetrazole-TtR_3 (Tt = C, Si; R = H, F). Promotion of SiR_3 Transfer by a Triel Bond. *Phys. Chem. Chem. Phys.* **2022**, *24*, 25895–25903. [CrossRef] [PubMed]
28. Voronkov, A.M.G.; Grebneva, E.A.; Trofimova, O.M.; Chernov, N.F.; Albanov, A.I.; Chipanina, N.N. The Unusual Reaction of Phenyltrifluorosilane with 2-Aminoethanol and its N-Methyl Derivatives. *Dokl. Chem.* **2006**, *409*, 139–141. [CrossRef]
29. Tamao, K.; Hayashi, T.; Ito, Y. Anion Complexation by Bidentate Lewis Acidic Hosts, Ortho-bis(fluorosilyl)benzenes. *J. Organomet. Chem.* **1996**, *506*, 85–91. [CrossRef]
30. Voronkov, M.G.; Trofimova, O.M.; Chernov, N.F.; Albanov, A.I.; Chipanina, N.N.; Grebneva, E.A. Reaction of Phenyltrifluorosilane with 8-Hydroxy- or 8-Mercapto-Quinoline and their Derivatives as a Route to New Heterocyclic Compounds of Pentacoordinate Silicon. *Appl. Organomet. Chem.* **2005**, *19*, 538–541. [CrossRef]
31. Nakash, M.; Gut, D.; Goldvaser, M. Formation of Hypervalent Complexes of Trifluorosilanes with Pyridine and with 4-Methoxypyridine, through Intermolecular Silicon···Nitrogen Interactions. *Inorg. Chem.* **2005**, *44*, 1023–1030. [CrossRef]
32. Kobelt, C.; Burschka, C.; Bertermann, R.; Guerra, C.F.; Bickelhaupt, F.M.; Tacke, R. Synthesis and Structural Characterisation of Neutral Pentacoordinate Silicon(iv) Complexes with a Tridentate Dianionic N,N,S Chelate Ligand. *Dalton Trans.* **2012**, *41*, 2148–2162. [CrossRef] [PubMed]
33. Sohail, M.; Panisch, R.; Bowden, A.; Bassindale, A.R.; Taylor, P.G.; Korlyukov, A.A.; Arkhipov, D.E.; Male, L.; Callear, S.; Coles, S.J.; et al. Pentacoordinate Silicon Complexes with Dynamic Motion Resembling a Pendulum on the S_N2 Reaction Pathway. *Dalton Trans.* **2013**, *42*, 10971–10981. [CrossRef] [PubMed]
34. Liu, N.; Wu, Q.Z.; Li, Q.Z.; Scheiner, S. Promotion of TH_3 (T = Si and Ge) Group Transfer within a Tetrel Bond by a Cation–π Interaction. *Phys. Chem. Chem. Phys.* **2022**, *24*, 1113–1119. [CrossRef] [PubMed]
35. Liu, N.; Xie, X.Y.; Li, Q.Z.; Scheiner, S. Enhancement of the Tetrel Bond by the Effects of Substituents, Cooperativity, and Electric Field: Transition from Noncovalent to Covalent Bond. *ChemPhysChem* **2021**, *22*, 2305–2312. [CrossRef] [PubMed]
36. Bundhun, A.; Ramasami, P.; Murray, J.S.; Politzer, P. Trends in σ-Hole Strengths and Interactions of F_3MX Molecules (M = C, Si, Ge and X = F, Cl, Br, I). *J. Mol. Model.* **2013**, *19*, 2739–2746. [CrossRef]
37. Scheiner, S. Highly Selective Halide Receptors Based on Chalcogen, Pnicogen, and Tetrel Bonds. *Chem. Eur. J.* **2016**, *22*, 18850–18858. [CrossRef]
38. Boys, S.F.; Bernardi, F. The Calculation of Small Molecular Interactions by the Differences of Separate Total Energies. Some Procedures with Reduced Errors. *Mol. Phys.* **1970**, *19*, 553–566.
39. Frisch, M.J.; Trucks, G.W.; Schlegel, H.B. *Gaussian 09, Revision A.02*; Gaussian, Inc.: Wallingford, UK, 2009.
40. Bulat, F.A.; Toro-Labbé, A.; Brinck, T.; Murray, J.S.; Politzer, P. Quantitative Analysis of Molecular Surfaces: Areas, Volumes, Electrostatic Potentials and Average Local Ionization Energies. *J. Mol. Model.* **2010**, *16*, 1679–1691. [CrossRef]
41. Lu, T.; Chen, F.W. Multiwfn: A Multifunctional Wavefunction Analyzer. *J. Comput. Chem.* **2012**, *33*, 580–592. [CrossRef]
42. Bader, R.F.W. *Atoms in Molecules*; A Quantum Theory; Clarendon: Oxford, UK, 1990.
43. Reed, A.E.; Curtiss, L.A.; Weinhold, F.A. Intermolecular Interactions from a Natural Bond Orbital, Donor-Acceptor Viewpoint. *Chem. Rev.* **1988**, *88*, 899–926. [CrossRef]
44. Mitoraj, M.P.; Michalak, A.; Ziegler, T. A Combined Charge and Energy Decomposition Scheme for Bond Analysis. *J. Chem. Theory Comput.* **2009**, *5*, 962–975. [CrossRef] [PubMed]
45. Su, P.F.; Li, H. Energy Decomposition Analysis of Covalent Bonds and Intermolecular Interactions. *J. Chem. Phys.* **2009**, *131*, 014102. [CrossRef]
46. Schmidt, M.W.; Baldridge, K.K.; Boatz, J.A.; Elbert, S.T.; Gordon, M.S.; Jensen, J.H.; Koseki, S.; Matsunaga, N.; Nguyen, K.A.; Su, S.J.; et al. General Atomic and Molecular Electronic Structure System. *J. Comput. Chem.* **1993**, *14*, 1347–1363. [CrossRef]
47. Arnold, W.D.; Oldfield, E. The Chemical Nature of Hydrogen Bonding in Proteins via NMR: J-Couplings, Chemical Shifts, and AIM Theory. *J. Am. Chem. Soc.* **2000**, *122*, 12835–12841. [CrossRef]
48. Zhuo, H.Y.; Jiang, L.X.; Li, Q.Z.; Li, W.Z.; Cheng, J.B. Is There an Attractive Interaction between Two Methyl Groups? *Chem. Phys. Lett.* **2014**, *608*, 90–94. [CrossRef]
49. Daolio, A.; Scilabra, P.; Terraneo, G.; Resnati, G. C(sp^3) Atoms as Tetrel Bond Donors: A Crystallographic Survey. *Coord. Chem. Rev.* **2020**, *413*, 213265. [CrossRef]
50. Southern, S.A.; West, M.S.; Bradshaw, M.J.Z.; Bryce, D.L. Experimental ^{13}C and ^{1}H Solid-State NMR Response in Weakly Tetrel-Bonded Methyl Groups. *J. Phys. Chem. C* **2021**, *125*, 2111–2123. [CrossRef]

51. Esrafili, M.D.; Asadollahi, S.; Mousavian, P. Anionic Tetrel Bonds: An ab Initio Study. *Chem. Phys. Lett.* **2018**, *691*, 394–400. [CrossRef]
52. Xu, H.L.; Cheng, J.B.; Li, H.B.; Yang, X.; Li, Q.Z. Tetrel bonds between $PhSiF_3$/$PhTH_3$ (T = Si, Ge, Sn) and H_3ZO (Z = N, P, As): A Pentacoordinate Silicon (IV) Complex. *Int. J. Quantum Chem.* **2018**, *118*, e25660. [CrossRef]
53. Xu, H.L.; Cheng, J.B.; Yu, X.F.; Li, Q.Z. Abnormal Tetrel Bonds between Formamidine and TH_3F: Substituent Effects. *ChemistrySelect* **2018**, *3*, 2842–2849. [CrossRef]
54. Zierkiewicz, W.; Michalczyk, M.; Scheiner, S. Implications of Monomer Deformation for Tetrel and Pnicogen Bonds. *Phys. Chem. Chem. Phys.* **2018**, *20*, 8832–8841. [CrossRef] [PubMed]
55. Zierkiewicz, W.; Michalczyk, M. On the Opposite Tends of Correlations between Interaction Energies and Electrostatic Potentials of Chlorinated and Methylated Amine Complexes Stabilized by Halogen Bond. *Theor. Chem. Acc.* **2017**, *136*, 125. [CrossRef]
56. Sarwar, M.G.; Dragisic, B.; Salsberg, L.J.; Gouliaras, C.; Taylor, M.S. Thermodynamics of Halogen Bonding in Solution: Substituent, Structural, and Solvent Effects. *J. Am. Chem. Soc.* **2010**, *132*, 1646–1653. [CrossRef]
57. An, X.L.; Yang, X.; Li, Q.Z. Tetrel Bonds between Phenyltrifluorosilane and Dimethyl Sulfoxide: Influence of Basis Sets, Substitution and Competition. *Molecules* **2021**, *26*, 7231. [CrossRef]
58. Wei, Y.X.; Li, H.B.; Cheng, J.B.; Li, W.Z.; Li, Q.Z. Prominent Enhancing Effects of Substituents on the Strength of π···σ-Hole Tetrel Bond. *Int. J. Quantum Chem.* **2017**, *117*, e25448. [CrossRef]
59. Wei, Y.X.; Cheng, J.B.; Li, W.Z.; Li, Q.Z. Regulation of Coin Metal Substituents and Cooperativity on the Strength and Nature of Tetrel Bonds. *RSC Adv.* **2017**, *7*, 46321–46328. [CrossRef]
60. Liu, M.X.; Li, Q.Z.; Li, W.Z.; Cheng, J.B. Carbene Tetrel-Bonded Complexes. *Struct. Chem.* **2017**, *28*, 823–831. [CrossRef]

Disclaimer/Publisher's Note: The statements, opinions and data contained in all publications are solely those of the individual author(s) and contributor(s) and not of MDPI and/or the editor(s). MDPI and/or the editor(s) disclaim responsibility for any injury to people or property resulting from any ideas, methods, instructions or products referred to in the content.